Journal of Alloys and Compounds 690 (2017) 8–14

Contents lists available at ScienceDirect

Journal of Alloys and Compounds

journal homepage: http://www.elsevier.com/locate/jalcom

Effect of synthesis on structure, oxygen voids, valence bands, forbidden band gap and magnetic domain configuration of La_2CoMnO_6

Hong Chang*, Yu Gao, Fang Liu, Yifan Liu, Hongjing Zhu, Yuehou Yun

School of Physics, Inner Mongolia University, Hohhot 010021, China

ARTICLE INFO

Article history:
Received 9 June 2016
Received in revised form
9 August 2016
Accepted 10 August 2016
Available online 12 August 2016

Keywords:
Oxide materials
Optical spectroscopy
Magnetization

ABSTRACT

La_2CoMnO_6 were prepared by the solid state reaction (SSR) and the sol-gel method (SGM). Compared to SSR, the SGM sample has a smaller lattice. The XPS spectra of O 1s core level of SGM show an extra peak at 533.16 eV, owing to the oxygen deficient region. The valence band of SGM moves to the low energy side by 0.36 eV, compared to that of SSR due to the holes generated by oxygen voids. The forbidden band gap energies are 1.78 eV and 1.93 eV for the SGM and the SSR samples, respectively. At low temperature, both the samples have multiple magnetic phases. Both of them have one ferromagnetic (FM) transition at 153 K and one antiferromagnetic (AFM) transition at 123 K in common, and a spin glass state below 75 K is confirmed. Furthermore, SSR has one extra FM transition at 223 K, while SGM does not have. A magnetic configuration as … spin glass↓ - ↓AFM↓- ↑FM↑- ↓AFM↓- spin glass↓ … is proposed to interpret the magnetic properties. The existence of the AFM clusters and the coupling between the AFM cluster and the FM or the spin glass domains are confirmed by the low magnetization at 70 kOe, the high coercive field of over 10 kOe, and the existence of the magnetic exchange bias.

1. Introduction

Double perovskite La_2CoMnO_6 has attracted intensive attention by investigating the magnetic, dielectric and electronic phases in strongly correlated systems. La_2CoMnO_6 was reported to form perovskite related phases including orthorhombic (space group Pbnm) or rhombohedral (R-3c) structure. Bull et al. illustrated that the Co/Mn in La_2CoMnO_6 is long-range ordered, and the space group is $P2_1/n$ with the rocksalt-type Co/Mn atomic configuration [1,2]. The slight tilting of the BO6 and B'O6 octahedra of $A_2BB'O_6$ in different ways results in different magnetic phases [3]. Goodenough et al. reported that La_2CoMnO_6 is ferromagnetic (FM) with the Curie temperature at 226 K [4,5]. Blasse suggested that the Co^{2+}–O–Mn^{4+} superexchange in the rocksalt-type structure is the origin of the ferromagnetism [6]. The magnetic properties were influenced by different annealing atmospheres. After annealing in Ar, a metamagnetic transition is observed, and after annealing in O_2, the Curie temperature increases, and the magnetic transition temperature decreases while quenching induces lots of defects and disorders [7]. Sayed et al. also proposed that the annealing atmosphere has great influence on the magnetic properties of La_2CoMnO_6 [8]. The super-paramagnetism was observed in microwave sintered La_2CoMnO_6 nanoparticles [9]. As shown above, the properties of La_2CoMnO_6 are sensitive to different preparing conditions. It is generally accepted that the sample prepared by the sol-gel method, referred to as the SGM sample has better homogeneity than its peer sample prepared by the solid state reaction, referred to as the SSR sample in the text. Furthermore, negative magnetizations are observed but ignored by some researchers [8]. Generally, the negative magnetization is observed in antiferromagnetic (AFM)/FM multilayer thin film with magnetic coupling effect, which is usually accompanied with the exchange bias effect as used in spin valves and tunneling devices [10]. In this paper, we investigate the structural, the optical and the magnetic properties of the La_2CoMnO_6 compound prepared by SGM and SSR, including the crystal structure, the valences of the ions, the valence bands, the forbidden band gaps, and the magnetic properties.

2. Experiments

La_2CoMnO_6 were prepared by both the sol-gel method (SGM)

---

* Corresponding author.
E-mail address: changhong@imu.edu.cn (H. Chang).

http://dx.doi.org/10.1016/j.jallcom.2016.08.086

and the solid-state reaction (SSC). As preparing the SGM sample, $La(NO_3)_3 \cdot 6H_2O$, $Co(NO_3)_2$ and $Mn(NO_3)_4$ were used as the starting materials in the SGM sample. The stoichiometric quantities of the salts were dissolved in deionized water and then 1.5 times of the stoichiometric amount of citric acid was added to the stirring solution to get complete chelation. After 2-h stirring, the chelation was heated to 200 °C to allow the chelates to undergo polyesterification as well as to remove the excess water. The resulting gels were completely dried in an oven, ground and decomposed in air at 400 °C for 24 h. The products were annealed at 1300 °C for 12 h. The SSR sample was prepared with the starting materials La_2O_3, Gd_2O_3 and CoO with proper weights. The starting materials were ground in an agate mortar, and heated at 850 °C in air for 12 h. Then the obtained powder was reground and fired at 1300 °C for 24 h. Powder x-ray diffraction (XRD) measurements were carried out using Rigaku D/max2500 powder X-ray diffraction with Cu K_α radiation. The diffraction data were collected for structure analysis, and the scan range 2θ was from 5° to 80°, with a scanning step of $2\theta = 0.01°$ and a sampling time of 1 s. The X-ray photoelectric spectroscopy (XPS) is used to investigate the surface element concentration. XPS was carried out on Thermo escalab 250Xi with Al K_α photons (μ_B) and a hemispherical energy analyzer. The binding energy was calibrated using the C 1s level (248.6 eV) of the Carbon contamination. The ultraviolet–visible (UV–vis) spectroscopies of the samples were obtained using a PerkinElmer Lambda750 UV–visible spectrophotometer at room temperature in the wavelength from 200 nm to 800 nm with the sampling pitch at 2 nm. The magnetization was measured with a Quantum Design Physical Properties Measurement System in the temperature range of 5–300 K.

3. Results and discussion

3.1. Structure analysis

The XRD patterns of the SGM and the SSR samples are refined with the space group Pnma, as shown in Fig. 1 for the SGM sample as an example, with La at the 4c site, Co at the 4b site, and O at the 4c and the 8d sites (the XRD pattern of the SSR sample are provided in the supporting information). The parameters are listed in Table 1. The SSR sample has expanded lattice with a = 5.481336 (120) Å, b = 7.768152 (172) Å, c = 5.522943 (119) Å, than its peer SGM sample with a = 5.472896 (90) Å, b = 7.755580 (122) Å, c = 5.518549 (85) Å, by 0.16% along the a and the b axis, and 0.08% along the c axis. With the same starting material, the different lattice leads to a possible indication that the oxygen content may be different in the SSR and the SGM samples. As there are enough oxygen voids, La_2CoMnO_5 with less oxygen content is also a candidate structure. The brownmillerite-type La_2CoMnO_5 structure is composed of single layers of corner-sharing CoO_6-octahedra connected by layers of CoO_4-tetrahedra running along [100]. The space group is Pnma, and La locates at the 8d, Co at the 4a and 4c and O at the 8d, 8d and 4c sites. The parameters are also listed in Table 1, and the refined xrd patterns of the SSR and the SGM samples with the brownmillerite-type La_2CoMnO_5 structure are provided in the supporting information. The reliability factors, Rwp, Rexp and χ^2 of the two kinds of structure have similar values, and both are acceptable. We adopt the first one without the ordered alignment of oxygen voids. Even though the composition and the structure may not form the double layered La_2CoMnO_5 with less oxygen, oxygen voids are allowed to be in the crystal. The oxygen contents obtained from the refined XRD patterns are 2.66 and 2.83 for the SGM and the SSR samples. The SGM sample has a higher oxygen content than the SSR sample does. The nearest Co–O bond length increases from 1.849 Å for the SSR sample to 1.957 Å for the SGM sample, while the next and the 3rd nearest Co–O distances of the SGM sample decrease. It does not change following the variation of the lattice. The Co–O–Co bond angles change from 135.40°, 165.93°, and 146.61° for the SSR sample to 103.93°, 164.61° and 156.07° for the SGM sample, as listed in Table 2. The varied Co–O–Co bond lengths and the deviation of the Co–O–Co angles (165.93° and 164.61° for the SSR and the SGM samples) from 180° give a clear view that the CoO6 octahedron is severely tilted due to the strain/stress in the lattice induced by the oxygen voids. The magnetic properties have a significant influence on the tilted CoO6 octahedron as illustrated in section 3.4.

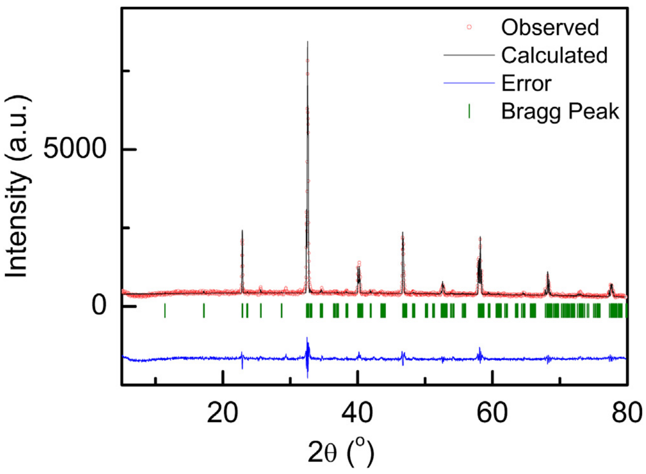

Fig. 1. xrd diffraction patterns of the SGM sample, with the red point as the experimental data, the black line as the refined pattern, the green ticks as the Bragg position, and the blue curve as the difference between the experimental and the refined curves. (For interpretation of the references to colour in this figure legend, the reader is referred to the web version of this article.)

3.2. XPS spectra

Fig. 2(a)–(c) show the XPS spectra of the Co 2p, Mn 2p, O 1s core level, with the binding energy were aligned with respect to C 1s peak (284 eV). The Co 2p core level regions were fitted, with 2 peaks at 779.60 eV and 780.66 eV, which are corresponding to Co^{2+} and Co^{3+} oxidation states, respectively. The Mn 2p core level regions were fitted with 642.37 eV for Mn^{4+} and 641.26 eV for Mn^{3+}. In the upper figure of Fig. 2(c) for the SSR sample, the XPS spectra of O 1s core level have 2 peaks at 529.38 eV and 531.66 eV. The peak at 529.38 eV is associated with the lattice oxygen, and the other at 531.66 eV due to the absorbed oxygen [11,12]. In the SGM sample, besides the 2 peaks, there is one extra peak at about 533.16 eV. The peak also appears in the sol-gel La_2CoMnO_6/CeO_2 sample [13], and it is attributed to the contribution of the oxygen deficient regions. Fig. 2(d) shows the XPS valence band spectra of the SGM and the SSR samples. The structures A, B, C, D and E are attributed to Co 3d, Mn 3d electrons, and Co 3d − O 2p and Mn 3d − O 2p bonding states [14]. Compared to the SSR sample, the structures of the SGM sample move to the low energy side. The energy differences between the valence band energy and the Fermi energy are 0.10 eV and 0.46 eV for the SGM and the SSR samples. In La_2CoMnO_6, the hole could be created accompanied by loss of oxygen, according to O_x - > $V_o + 1/2O_2 + h$. The lowered energy difference demonstrates that the hole concentration increase in the SGM sample.

3.3. UV–vis spectroscopy

Assuming that the nature of the sample transition as direct